Multimode Equivalent Network Representation for *H*- and *E*-Plane Uniform Bends in Rectangular Waveguide

Benito Gimeno and Marco Guglielmi

Abstract— **Uniform bends in rectangular waveguides are frequently used components in many microwave subsystems both for ground and space applications. Their accurate and efficient full-wave characterization is therefore required for the development of modern CAD tools to analyze and design complex waveguide structures. In this paper we describe new multimode network representations for both *H*- and *E*-plane uniform bends in terms of impedance and admittance multimode coupling matrices, respectively. The key element of the network is the transition from the straight waveguide to the curved waveguide. The relevant multimode equivalent network representation is obtained following a simple procedure that has already been used with success for other types of junctions involving straight waveguides. The convergency properties of the method are discussed, and comparisons between our simulations and theoretical and experimental data are presented, indicating that the approach proposed is at the same time accurate and computationally very efficient.**

I. Introduction

UNIFORM bends in rectangular waveguides, like the ones shown in Fig. 1, are frequently used components in many microwave subsystems both for ground and space applications. Their accurate and efficient full-wave characterization is therefore required for the development of modern CAD tools to analyze and design complex waveguide structures. Several contributions can be found in the technical literature concerning bends. Starting with early contributions, Rice [1] obtains two approximate formulas for the reflection coefficient of the *H*- and *E*-plane bends with large radius of curvature. Cochran [2] presents results of the propagation constants of *H*- and *E*-plane bends as function of several parameters, expanding the radial component of the electric and magnetic fields as a combination of Bessel functions. Bates [3] analyzes the junction between straight and curved waveguides with a method based on an integral equation formulation. Lewin [4] derives approximate modal solutions for *H*- and *E*-plane bends by means of a perturbation analysis. More recently, Carle [5] presented a single-mode circuit for *E*-plane bends. Accatino [6] applied mode-matching technique to analyze *H*- and *E*-plane bends, using an ad-hoc solution of the characteristic equation (which involves Bessel functions), allowing him to bypass the ill-conditioning of the problem for the propagation constants in the curved region. Weisshaar [7] presented an accurate method based on mode-matching technique where the Helmholtz equation in the curved region is transformed into an eigenvalue problem. Most of the above publications are based on mode matching technique (except for [5] where a single-mode equivalent network is presented) and give scattering parameter representations.

Recently, modern CAD tools for complex waveguide systems have been developed which are based on admittance or impedance multimode network representations (see for instance [8], [9]). Thus, the objective of this paper is to describe multimode equivalent network representations for both *H*- and *E*-plane uniform bends in terms of impedance and admittance multimode coupling matrices, respectively. The key element of the network is the transition from the straight waveguide to the curved waveguide regions [10]. The details of the formulations are given in this paper with comparisons between our simulations and available published data, both measured and theoretical. The convergence of the method is also analyzed, indicating very good behavior as well as very good computational efficiency.

II. Theory

A. H-Plane Bend

The viewpoint chosen to simulate the waveguide bend shown in Fig. 1(a) consists in cascading two discontinuities through a length $S = R\phi$ of uniformly curved waveguide, obtaining the multimode equivalent network representation shown in Fig. 2. The key discontinuities are then the junctions between straight to curved and curved to straight waveguide regions. Once the problem has been decomposed in this fashion, the first step toward the development of the multimode equivalent network representation is the computation of an orthonormal set of modes for the curved waveguide region. The procedure chosen to obtain the appropriate modal decomposition is based on a combination of [4] and [7], and is outlined below.

We begin with the expansion of the transverse electric and magnetic fields in the curved region as an infinite series of modes

$$\mathbf{E}_t^{(c)} = \sum_{m=1}^{+\infty} V_m^{(c)} \mathbf{e}_m^{(c)} \tag{1}$$

$$\mathbf{H}_t^{(c)} = \frac{1}{1+\frac{x}{R}} \sum_{m=1}^{+\infty} I_m^{(c)} \mathbf{h}_m^{(c)} \tag{2}$$

Manuscript received September 22, 1995; revised June 14, 1996.

B. Gimeno was with the European Space Research and Technology Centre (ESTEC), 2200 AG Noordwijk, The Netherlands, on leave from the Departamento de Fisica Aplicada, Universidad de Valencia, 46100 Burjasot Valencia, Spain.

M. Guglielmi is with the European Space Research and Technology Centre (ESTEC), 2200 AG Noordwijk, The Netherlands.

Publisher Item Identifier S 0018-9480(96)06904-9.

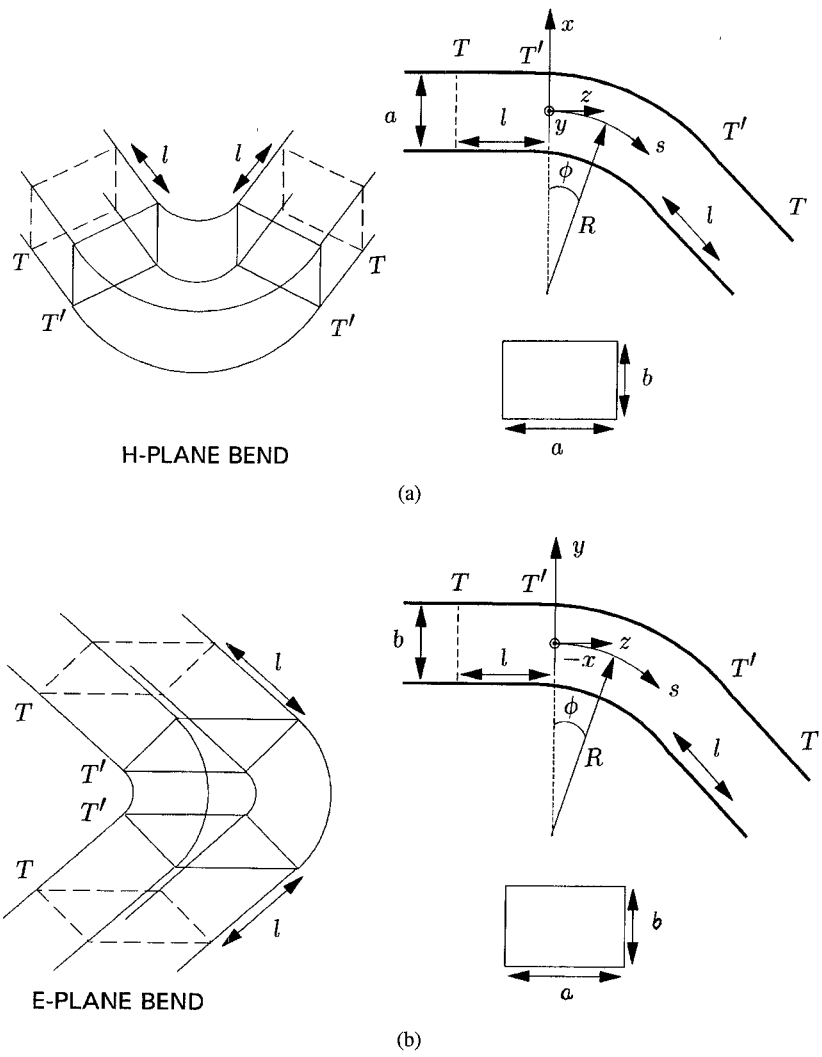

Fig. 1. Uniform H- and E-plane bends in rectangular waveguide.

where the superscripts (c) denotes the curved region. Each mode of the curved region ($\mathbf{e}_m^{(c)}$ and $\mathbf{h}_m^{(c)}$) is then expanded into an infinite series of standard parallel-plate waveguide basis functions $\mathbf{e}_n^{(s)}$, $\mathbf{h}_n^{(s)}$, namely [see Fig. 1(a)]

$$\mathbf{e}_m^{(c)} = -\sum_{n=1}^{+\infty} d_n^{(m)} \mathbf{e}_n^{(s)} \tag{3}$$

$$\mathbf{h}_m^{(c)} = -\sum_{n=1}^{+\infty} d_n^{(m)} \mathbf{h}_n^{(s)} \tag{4}$$

with

$$\mathbf{e}_n^{(s)} = -\sqrt{\frac{2}{a}} \sin\left(\frac{n\pi}{a}\left(x + \frac{a}{2}\right)\right)\mathbf{y_0}; \quad n = 1, 2, 3 \ldots \tag{5}$$

$$\mathbf{h}_n^{(s)} = \sqrt{\frac{2}{a}} \sin\left(\frac{n\pi}{a}\left(x + \frac{a}{2}\right)\right)\mathbf{x_0}; \quad n = 1, 2, 3 \ldots \tag{6}$$

where the superscript (s) denotes the straight region. The series (3) and (4) are then inserted in the Helmholtz equation of the curved region, obtaining a matrix eigenvalue problem (see details in Appendix A). The following inner products, called in the remainder the overlapping integrals, are required in this procedure

$$\langle f, g \rangle^{(c)} = \int_{-a/2}^{a/2} \frac{1}{1 + \frac{x}{R}} f(x) g(x) dx \tag{7}$$

$$\langle f, g \rangle^{(s)} = \int_{-a/2}^{a/2} f(x) g(x) dx. \tag{8}$$

Finally, the linear matrix eigenvalue problem is solved, and the propagation constants $\beta_m^{(c)}$ and the coefficients of the series expansion $d_n^{(m)}$ are obtained numerically. The characteristic impedances associated with these modes are

$$Z_n^{(s)} = \frac{\omega \mu_0}{\beta_n^{(s)}} \tag{9}$$

$$\beta_n^{(s)} = \sqrt{\omega^2 \mu_0 \varepsilon_0 - \left(\frac{n\pi}{a}\right)^2} \tag{10}$$

$$Z_m^{(c)} = \frac{\omega \mu_0}{\beta_m^{(c)}}. \tag{11}$$

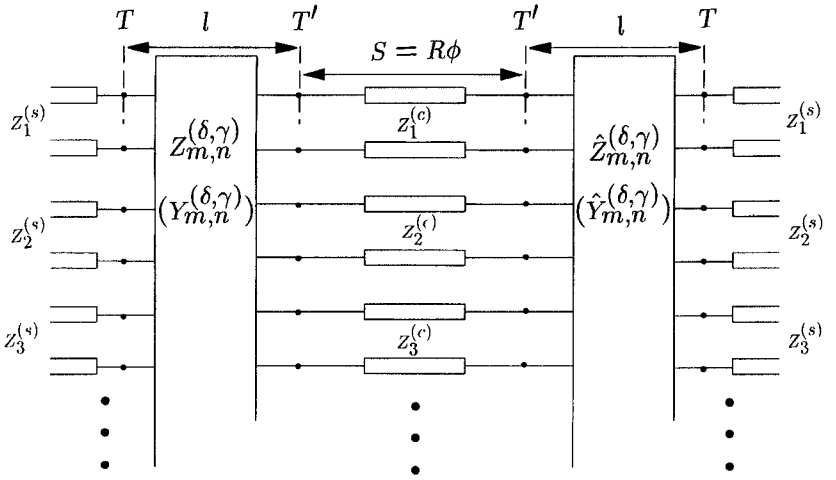

Fig. 2. Multimode equivalent network for H- and E-plane bends. The $Z_{m,n}^{(\gamma,\delta)}(Y_{m,n}^{(\gamma,\delta)})$and $\hat{Z}_{m,n}^{(\gamma,\delta)}(\hat{Y}_{m,n}^{(\gamma,\delta)})$ impedance (admittance) matrices represent the transition from the straight to the curved and the curved to the straight waveguide regions, respectively. The transmission line of length S represents the propagation in the curved waveguide region.

It is important to note that the following orthonormalization condition is satisfied automatically, because of a property of the diagonalization process to obtain the modes of the curved region

$$\langle \mathbf{e}_m^{(c)}, \mathbf{e}_n^{(c)} \rangle^{(c)} = \langle \mathbf{h}_m^{(c)}, \mathbf{h}_n^{(c)} \rangle^{(c)} = \delta_{m,n}. \tag{12}$$

The vector mode functions of the straight waveguide region also satisfy an orthonormalization condition, namely

$$\langle \mathbf{e}_m^{(s)}, \mathbf{e}_n^{(s)} \rangle^{(s)} = \langle \mathbf{h}_m^{(s)}, \mathbf{h}_n^{(s)} \rangle^{(s)} = \delta_{m,n}. \tag{13}$$

Once the modes of the curved waveguide region are obtained, the next step is to analyze the junction between the straight and the curved waveguide regions. This has been done adapting a simple method that has already been used to analyze the junction between arbitrary straight waveguides [11]. To proceed we need to define two reference planes denoted as T and T', as shown in Fig. 1. The plane T' is at the junction between the two waveguide regions, while the plane T is located at a distance l in the straight waveguide. We can then write the mathematical equivalent of the network representation between the reference planes T and T', represented as a multiport in Fig. 2, in the form

$$V_m^{(\delta)} = \sum_{n=1}^{+\infty} Z_{m,n}^{(\delta,s)} I_n^{(s)} + \sum_{n=1}^{+\infty} Z_{m,n}^{(\delta,c)} I_n^{(c)};\ (\delta) = (c), (s) \tag{14}$$

where $V_m^{(\delta)}$ and $I_m^{(\delta)}$ are the modal voltages and currents, respectively. According to circuit theory, the $Z_{m,n}^{(\delta,\gamma)}$ element is given by the general relation

$$Z_{m,n}^{(\delta,\gamma)} = \left. \frac{V_m^{(\delta)}}{I_n^{(\gamma)}} \right| I_k^{(\xi)} = 0 \ \ \forall\, \xi \neq \gamma \quad \text{and } k \neq n. \tag{15}$$

This relation can be interpreted as follows: place an open-circuit in all ports with the exception of the exciting port (γ) where only the current $I_n^{(\gamma)}$ is supposed to be incident, and evaluate the voltage $V_m^{(\delta)}$ on the open-circuited port (δ). Expression (15) can be actually used to evaluate the $Z_{m,n}^{(\delta,\gamma)}$ elements obtaining the general expression

$$Z_{m,n}^{(\delta,\gamma)} = \frac{\langle \mathbf{E}(I_n^{(\gamma)}), \mathbf{e}_m^{(\delta)} \rangle^{(\delta)}}{I_n^{(\gamma)}} \tag{16}$$

where $\mathbf{E}(I_n^{(\gamma)})$ is the electric field excited in the open-circuited port (δ) when only the nth mode is incident in the port (γ), and the inner product is evaluated in the region corresponding to the port (δ).

Starting with $Z_{m,n}^{(s,s)}$, we put an open-circuit in T' obtaining the equivalent transmission line representation in Fig. 3(a), so that we can write directly

$$Z_{m,n}^{(s,s)} = -jZ_m^{(s)} \cot\left(\beta_m^{(s)} l\right) \delta_{m,n}. \tag{17}$$

Before proceeding further, we recall that the expression relating the current to the voltage along an open-circuit transmission line is given by

$$V(z) = -jZ_0 I(z)|_{z=-l} \cos(\beta z) \csc(\beta l) \tag{18}$$

Z_0 being the characteristic impedance of the line. Following the general relation (16), then we have [see Fig. 3(a)]

$$Z_{m,n}^{(s,c)} = Z_{n,m}^{(c,s)} = jZ_n^{(s)} \csc\left(\beta_n^{(s)} l\right) \langle \mathbf{e}_n^{(s)}, \mathbf{e}_m^{(c)} \rangle^{(c)} \tag{19}$$

where the inner product is given by

$$\langle \mathbf{e}_n^{(s)}, \mathbf{e}_m^{(c)} \rangle^{(c)} = -\sqrt{\frac{2}{a}} \sum_r d_r^{(m)} \int_{-a/2}^{a/2} \frac{1}{1+\frac{x}{R}} \times \sin\left(\frac{n\pi}{a}\left(x+\frac{a}{2}\right)\right) \sin\left(\frac{r\pi}{a}\left(x+\frac{a}{2}\right)\right) dx. \tag{20}$$

The last element to be determined is $Z_{m,n}^{(c,c)}$. The reference system used to evaluate this element has to be inverted, as it is shown in Fig. 3(b). Now, we place in T an open-circuit and suppose that the single mode $I_n^{(c)}$ is incident from the curved

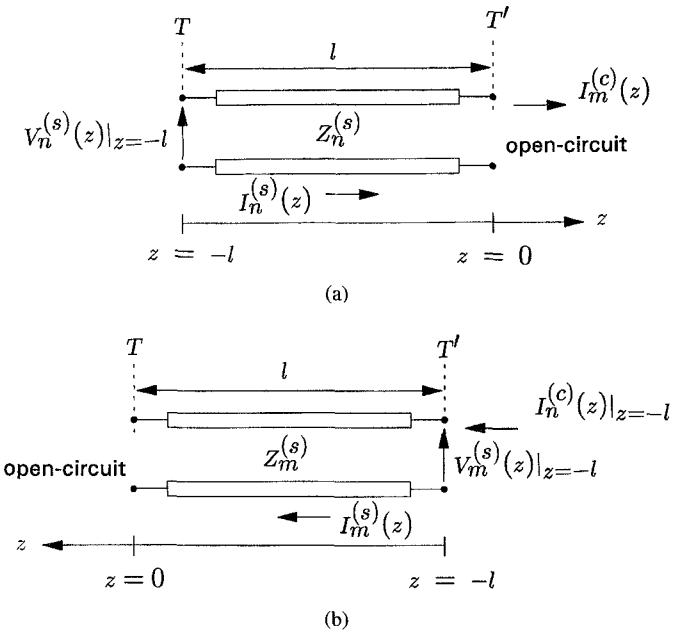

Fig. 3. Length of open-circuited transmission line to evaluate the elements $Z_{m,n}^{(\delta,\gamma)}$ of the impedance matrix.

region. Denoting as $\mathbf{H}_n^{(s)}(z)|_{z=-l}$ the magnetic field in the T' plane, we can write

$$\mathbf{H}_n^{(s)}(z)\big|_{z=-l} = \frac{1}{1+\frac{x}{R}} I_n^{(c)} \mathbf{h}_n^{(c)} \tag{21}$$

This magnetic field excites all modes of the cavity defined between the planes T and T', and the expansion coefficients of these modes can be obtained as follows:

$$I_k^{(s)} = \left\langle \frac{1}{1+\frac{x}{R}} I_n^{(c)} \mathbf{h}_n^{(c)}, \mathbf{h}_k^{(s)} \right\rangle^{(s)}. \tag{22}$$

Now, in order to apply the general relation (16), the tangential electric field in the straight waveguide cavity in the T' plane, denoted as $\mathbf{E}_n^{(s)}(z)\,|_{z=-l}$, has to be calculated, obtaining

$$\mathbf{E}_n^{(s)}(z)\big|_{z=-l} = \sum_{k=1}^{+\infty} -jZ_k^{(s)} \cot\left(\beta_k^{(s)} l\right) I_k^{(s)} \mathbf{e}_k^{(s)} \tag{23}$$

and finally we obtain the expression for $Z_{m,n}^{(c,c)}$, namely

$$Z_{m,n}^{(c,c)} = -j \sum_{k=1}^{+\infty} Z_k^{(s)} \cot\left(\beta_k^{(s)} l\right) \left\langle \mathbf{e}_k^{(s)}, \mathbf{e}_m^{(c)} \right\rangle^{(c)} \left\langle \frac{1}{1+\frac{x}{R}} \mathbf{h}_n^{(c)}, \mathbf{h}_k^{(s)} \right\rangle^{(s)} \tag{24}$$

where the second inner product is given by

$$\left\langle \frac{1}{1+\frac{x}{R}} \mathbf{h}_n^{(c)}, \mathbf{h}_k^{(s)} \right\rangle^{(s)} = -\sqrt{\frac{2}{a}} \sum_r d_r^{(n)} \int_{-a/2}^{a/2} \frac{1}{1+\frac{x}{R}} \times \sin\left(\frac{k\pi}{a}\left(x+\frac{a}{2}\right)\right) \sin\left(\frac{r\pi}{a}\left(x+\frac{a}{2}\right)\right) dx. \tag{25}$$

This concludes the derivation of the impedance matrix. What is important to note, is that the overlapping integrals involved in the process to obtain the elements of the impedance matrix are not frequency-dependent, and that only the $Z_{m,n}^{(c,c)}$ elements involve a summation.

Once the impedance matrix for the junction between straight and curved regions has been evaluated, the next step to simulate a complete bend is to obtain the impedance matrix corresponding to the transition from the curved to the straight waveguide regions. The elements of this matrix, denoted as $\hat{Z}_{m,n}^{(\gamma,\delta)}$ in Fig. 2, are then easily obtained taking account the physical symmetry of the structure, so that

$$\hat{Z}_{m,n}^{(\gamma,\delta)} = Z_{m,n}^{(\delta,\gamma)}. \tag{26}$$

B. E-Plane Bend

The expansion of the transverse electric and magnetic fields of the curved region used to analyze E-plane bends is given by [see Fig. 1(b)]

$$\mathbf{E}_t^{(c)} = \frac{1}{1+\frac{y}{R}} \sum_{m=1}^{+\infty} V_m^{(c)} \mathbf{e}_m^{(c)} \tag{27}$$

$$\mathbf{H}_t^{(c)} = \sum_{m=1}^{+\infty} I_m^{(c)} \mathbf{h}_m^{(c)}. \tag{28}$$

To expand the field in the curved region we have applied the same procedure that for H-plane bends. Therefore, each mode of the curved region is expanded as

$$\mathbf{e}_m^{(c)} = -\sum_{n=0}^{+\infty} d_n^{(m)} \mathbf{e}_n^{(s)} \tag{29}$$

$$\mathbf{h}_m^{(c)} = -\sum_{n=0}^{+\infty} d_n^{(m)} \mathbf{h}_n^{(s)} \tag{30}$$

where

$$\mathbf{e}_n^{(s)} = -\sqrt{\frac{\epsilon_n}{b}} \cos\left(\frac{n\pi}{b}\left(x+\frac{b}{2}\right)\right) \mathbf{y_0}; \quad n = 0, 1, 2 \ldots \tag{31}$$

$$\mathbf{h}_n^{(s)} = \sqrt{\frac{\epsilon_n}{b}} \cos\left(\frac{n\pi}{b}\left(x+\frac{b}{2}\right)\right) \mathbf{x_0}; \quad n = 0, 1, 2 \ldots \tag{32}$$

and ϵ_n is 1 if $n = 0$ and 2 if $n \neq 0$. The inner products are defined in the curved and the straight regions as follows:

$$\langle f, g \rangle^{(c)} = \int_{-b/2}^{b/2} \frac{1}{1+\frac{y}{R}} f(y) g(y) dy \tag{33}$$

$$\langle f, g \rangle^{(s)} = \int_{-b/2}^{b/2} f(y) g(y) dy. \tag{34}$$

Note that using these inner products definitions the orthonormality conditions (12) and (13) are satisfied as well. Details of the procedure are also found in Appendix A. The characteristic admittances of these modes are given by

$$Y_n^{(s)} = \frac{\omega^2 \mu_0 \varepsilon_0 - \left(\frac{\pi}{a}\right)^2}{\omega \mu_0 \beta_n^{(s)}} \tag{35}$$

$$\beta_n^{(s)} = \sqrt{\omega^2 \mu_0 \epsilon_0 - \left(\frac{\pi}{a}\right)^2 - \left(\frac{n\pi}{b}\right)^2} \tag{36}$$

$$Y_m^{(c)} = \frac{\omega^2 \mu_0 \varepsilon_0 - \left(\frac{\pi}{a}\right)^2}{\omega \mu_0 \beta_m^{(c)}} \tag{37}$$

where $\beta_m^{(c)}$ again represents the modal propagation constant in the curved waveguide and is obtained from the solution of the eigenvalue problem. Following [11] we can now write directly these expressions for the admittance matrix elements

$$Y_{m,n}^{(s,s)} = -jY_m^{(s)} \cot\left(\beta_m^{(s)} l\right) \delta_{m,n} \tag{38}$$

$$Y_{m,n}^{(s,c)} = Y_{n,m}^{(c,s)} = jY_n^{(s)} \csc\left(\beta_n^{(s)} l\right) \left\langle \mathbf{h}_n^{(s)}, \mathbf{h}_m^{(c)} \right\rangle^{(c)} \tag{39}$$

$$Y_{m,n}^{(c,c)} = -j \sum_{k=0}^{+\infty} Y_k^{(s)} \cot\left(\beta_k^{(s)} l\right) \left\langle \mathbf{h}_k^{(s)}, \mathbf{h}_m^{(c)} \right\rangle^{(c)} \times \left\langle \frac{1}{1+\frac{y}{R}} \mathbf{e}_n^{(c)}, \mathbf{e}_k^{(s)} \right\rangle^{(s)}. \tag{40}$$

C. Connection of Bends

Fig. 2 shows the equivalent network representation to simulate a complete bend. More complicated structures can be easily analyzed by connecting several equivalent network representations through appropriate transmission line lengths. Basically, there are two structures, called U- and S-configurations, respectively, which consist on connecting two bends through a length of straight rectangular waveguide. In the U-configuration the centers of curvature of the bends are in the same side, while in the S-configuration the centres of curvature are in opposite sides of the waveguide (see Fig. 4).

The equivalent network representation used to simulate the U-configuration is shown in Fig. 4(a). The negative lengths $-l$ and $-2l$ in the network are required in order to account for the length l as shown in Fig. 1.

In the S-configuration, since the centres of curvature are in opposite sides of the waveguide, a change of the reference frame is required [see Fig. 4(b)]. Let us denote with (x, y, s) and (x', y', s') the reference systems associated to the first and the second bends, respectively. In Fig. 4(b), a new "box" with dashed lines indicates the combined representation of the length of transmission line $L-2l$ with the change of reference frame required. To find the impedance matrix of this new element, the expression of the electric vector mode function in the prime system is changed to the nonprime frame, resulting for the H-plane case in the following expression:

$$\mathbf{e}_m^{(s)'} = -\sqrt{\frac{2}{a}} \sin\left(\frac{m\pi}{a}\left(-x+\frac{a}{2}\right)\right)(-\mathbf{y_0}) \tag{41}$$

where we have taken into account that $x = -x'$, $y = -y'$, $s = s'$. In order to find out the relationship between the modal voltages associated with the modes in both reference systems, we impose the continuity boundary condition of the transversal electric field in a plane located in the straight region in between the bends, obtaining

$$\sum_{n=1}^{+\infty} V_n \mathbf{e}_n^{(s)} = \sum_{m=1}^{+\infty} V_m' \mathbf{e}_m^{(s)'}. \tag{42}$$

After algebraic manipulations we find

$$V_n = \left\langle \sum_{m=1}^{+\infty} V_m' \mathbf{e}_m^{(s)'}, \mathbf{e}_n^{(s)} \right\rangle^{(s)} = (-1)^n V_n'. \tag{43}$$

A similar expression is found for the modal currents: $I_n = (-1)^n I_n'$. The change of the reference system must be included in the impedance matrix of the straight waveguide connecting the bends, the elements of this matrix are then given by

$$Z_{m,n}^{(1,1)} = Z_{m,n}^{(2,2)} = -jZ_m^{(s)} \cot\left(\beta_m^{(s)}(L-2l)\right)\delta_{m,n} \tag{44}$$

$$Z_{m,n}^{(2,1)} = Z_{m,n}^{(1,2)} = -j(-1)^m Z_m^{(s)} \csc\left(\beta_m^{(s)}(L-2l)\right)\delta_{m,n} \tag{45}$$

Similar expressions are obtained for the E-plane case.

Once the impedance (admittance) matrices of all elements of the structure are evaluated, they are properly connected to form a global multimode equivalent network. From the network, a band diagonal system is obtained, which has to be inverted in order to find the reflection and transmission coefficients of all modes. Thus, only one matrix inversion is required for each frequency point. This inversion is performed by means an adequate inversion algorithm for band diagonal systems [12], resulting in a very fast code implementation.

III. Numerical and Experimental Results

We are going to discuss the convergence of the expansions to describe the modes in the curved waveguide region. Fig. 5 shows the convergence of the propagation constants $\beta_m^{(c)}$ of the modes in the curved region as a function of the number of terms used to describe each mode. The summations (3) and (4) can be truncated to 20 terms to reach the region of convergency. In Fig. 6, the convergence of the element $Z_{3,3}^{(c,c)}$ as a function of the number of expansion terms is analyzed for different radii of curvature. The radii have been normalized with respect to the minimum radius possible $R_{\min} = \frac{a}{2}$. For small radius of curvature the convergence is slow and a large number of terms must to be included to achieve convergence, but for $R/R_{\min} > 1.4$ only 20 terms are enough to reach the region of convergence. Similar results are obtained for the E-plane case.

In Fig. 7 the convergence of the magnitude of the reflection coefficient with the number of modes in the global network is analyzed for both 90° H- and E-plane bends in WR-75 waveguide, showing that typically only 3 or 4 modes are required. The radius of curvature of the bends is 15 mm. Although 20 terms are strictly necessary to reach the region of convergency, we can see that only 10 expansion terms are enough to obtain an accurate solution in practical applications.

Next we compare our results with the ones presented by Weisshaar [7] in Fig. 8 for a S-configuration in the H-plane. As we can see, a very good agreement is observed. Finally, we present a comparison of the magnitude of the reflection coefficient and the phase of the transmission coefficient between measured results (courtesy of RYMSA) and our simulations in Fig. 9, for both H- and E-plane bends in WR-75 waveguide. Also in this case, the agreement is very good, thereby further validating the multimode equivalent network representation. The computation time for a typical analysis (with 3 modes in the network and 10 terms to describe each mode of the curved region) with 50 points in frequency is 1.6 seconds on a IBM RISK-6000 workstation. The computational effort is of

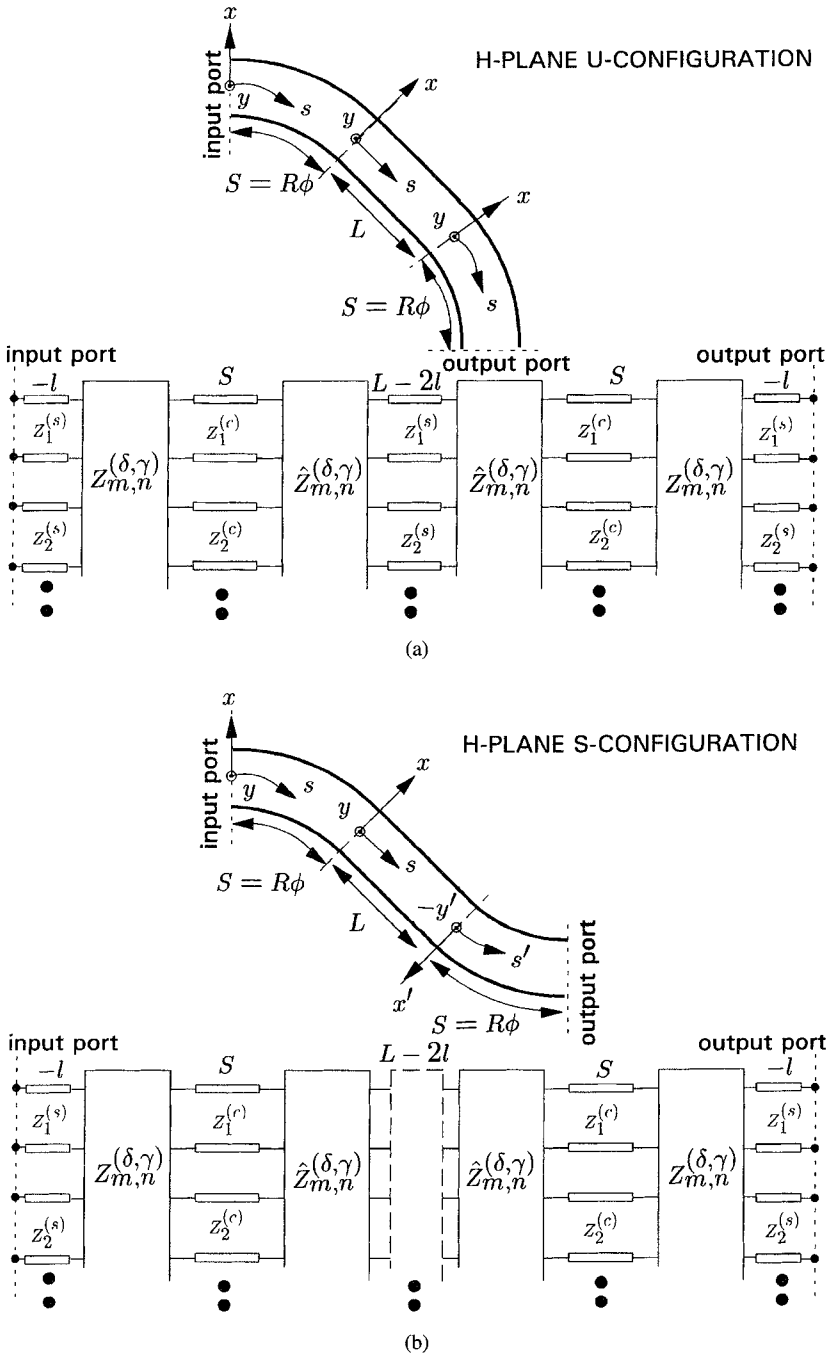

Fig. 4. U-and S- configurations of connected H-plane bends with the associated multimode equivalent network representations. For the S-configuration, the box with dashed lines combines the representation of the length of straight rectangular waveguide between the bends with the change of the reference system involved in this configuration.

the same order of magnitude of the ones required for other waveguide junctions commonly used in complex satellite microwave subsystems, and therefore the software developed in this paper can be easily integrated into existing CAD tools [9].

IV. Conclusion

A new multimode equivalent network representation for the analysis of uniform H- and E-plane bends in rectangular waveguide has been presented. The junction between straight and curved waveguide regions, which is the key element of the structure, is analyzed in terms of a multimode equivalent network representation involving an impedance or admittance coupling matrix for H- and E-plane bends, respectively. The convergence of the network representation has been analyzed as function of several parameters, showing very good behavior. Comparison with theoretical and experimental results fully validate the method presented. The value of the results presented is that the multimode network developed can now be easily inserted into existing CAD tools thereby allowing for the accurate analysis and design of more complex waveguide subsystems.

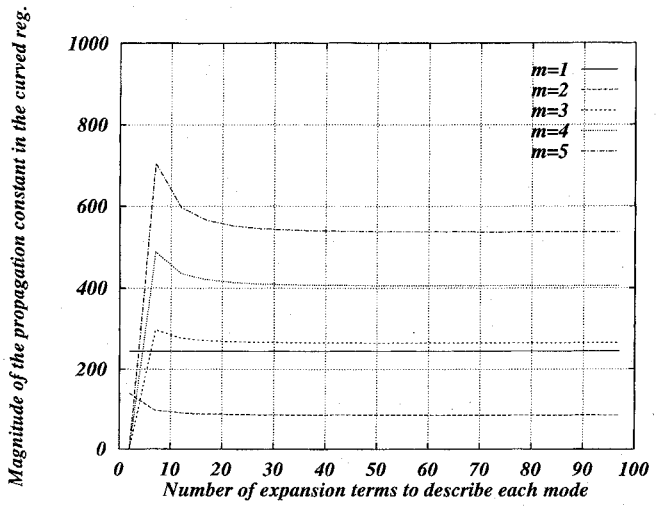

Fig. 5. Convergency of the propagation constant $\beta_m^{(c)}$ of the modes in the curved waveguide region as a function of the number of expansion terms used to describe each curved region mode (*H*-plane bend in WR-75 waveguide, $a = 10.050$ mm, $b = 9.525$ mm, radius $= 17$ mm, frequency $= 14$ GHz).

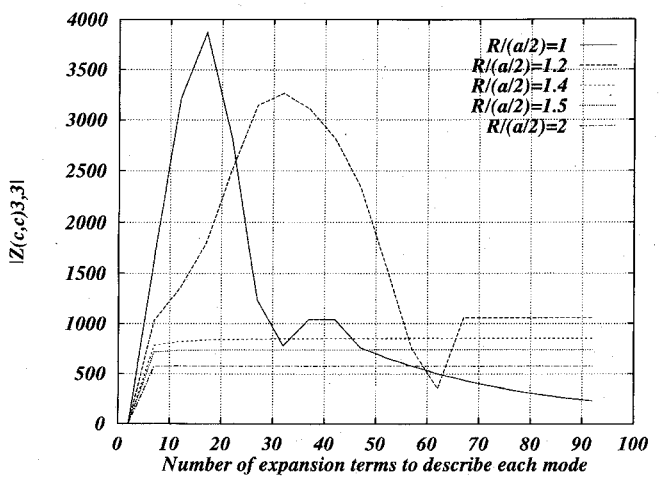

Fig. 6. Convergency of the element $Z_{3,3}^{(c,c)}$ as function of the number of expansion terms used to describe each curved region mode. The radius varies in order to analyze the convergence of the method as function of the curvature of the bend (*H*-planebend in WR-75 waveguide, $a = 10.050$ mm, $b = 9.525$ mm, frequency $= 14$ GHz).

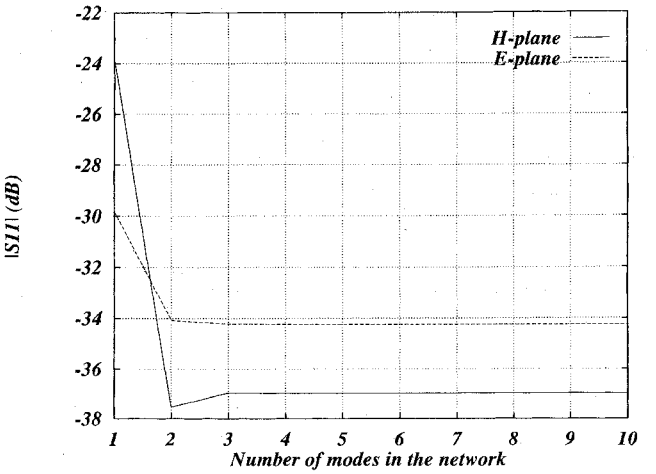

Fig. 7. Convergency of the magnitude of the reflection coefficient versus the number of modes included in the network. Ten expansion terms have been used to describe each curved region mode (90° *H*-plane and *E*-plane bends in WR-75waveguide, $a = 10.050$ mm, $b = 9.525$ mm, radius $= 15$ mm, frequency $= 15$ GHz).

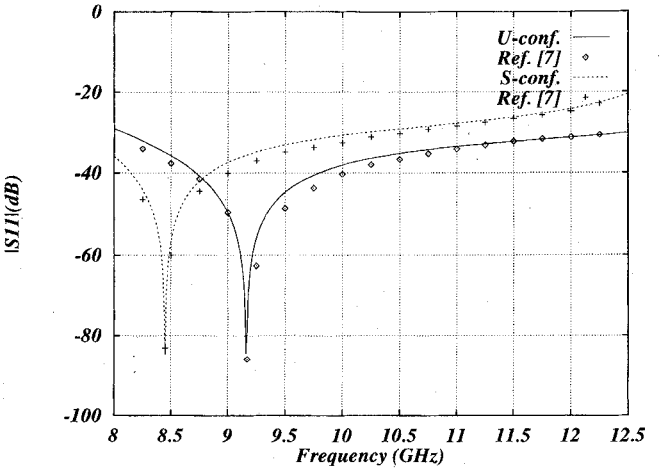

Fig. 8. Comparison of the results presented in Fig. 3(d) of [7] with our method. Cascaded 30° *H*-plane bends through a straight transmission line of length $L = 5$ mm. Ten expansion terms have been used to describe each curved region mode and three modes have been included in the network. Both *U*- and *S*-configurations have been analyzed. (WR-90 waveguide, $a = 22.900$ mm, $b = 10.200$ mm, radius $= 15.24$ mm).

APPENDIX A
MODAL SOLUTIONS IN THE CURVED WAVEGUIDE REGIONS

A. H-Plane Bends

Following Weisshaar [7], the Helmholtz equation in the *H*-plane curved region can be transformed by means of the Galerkin method into the following equivalent matrix eigenvalue problem

$$\sum_{i=1}^{N}\left(\left(\omega^2\mu\epsilon-\left(\frac{r\pi}{b}\right)^2\right)P_{ij}-S_{ij}\right)d_i^{(m)} = \beta_m^{(c)^2}\sum_{i=1}^{N}Q_{ij}d_i^{(m)};\quad j=1,2,\ldots,N. \tag{46}$$

It is important to note that this is a linear eigenvalue problem and can therefore be easily solved with standard mathematical routines for matrix operations.

If the TE_{10} rectangular waveguide mode is incident, only modes with $r = 0$ are excited in the curved region. The solution of the problem in (46) requires the computation of the elements of the matrices P_{ij}, S_{ij}, and Q_{ij}. The relevant explicit expressions (not given in [7]) are as follows:

$$P_{ij} = \frac{a}{2}\delta_{ij} + (1-\delta_{ij})\frac{1}{R}\frac{a^2}{2\pi^2} \times\left(\frac{(-1)^{i-j}-1}{(i-j)^2}-\frac{(-1)^{i+j}-1}{(i+j)^2}\right) \tag{47}$$

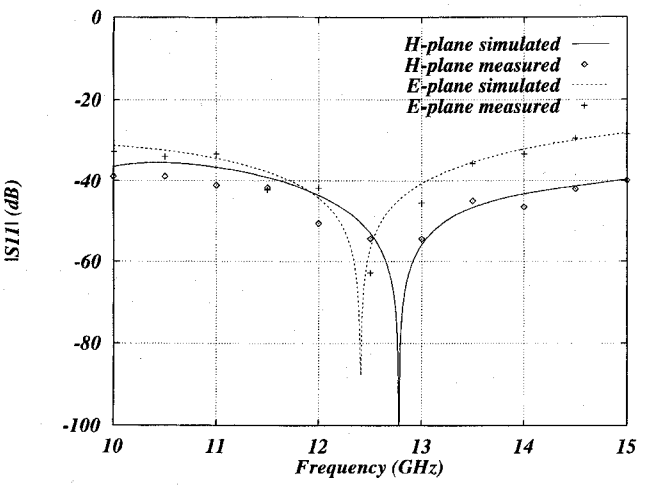

(a)

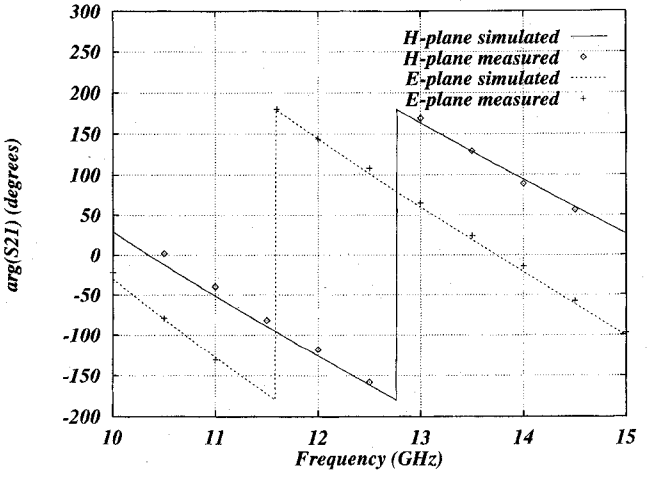

(b)

Fig. 9. Comparison between measured and simulation data. Ten expansion terms have been used to describe each curved region mode, and three modes have been included in the network. (a) Magnitude of the reflection coefficient, (b) phase of the transmission coefficient. Radius = 21.6mm and 12 mm for the H- and E-plane bends, respectively. (90° H- and E-plane bends in WR-75 waveguide, $a = 10.050$ mm, $b = 9.525$ mm).

$$S_{ij} = ij\left(\frac{\pi}{a}\right)^2\left(\frac{a}{2}\delta_{ij} + (1-\delta_{ij})\frac{1}{R}\frac{a^2}{2\pi^2} \times \left(\frac{(-1)^{i-j}-1}{(i-j)^2} + \frac{(-1)^{i+j}-1}{(i+j)^2}\right)\right) \quad (48)$$

$$Q_{ij} = \int_{-a/2}^{+a/2} \frac{R}{x+R}\sin\left(\frac{i\pi}{a}\left(x+\frac{a}{2}\right)\right) \times \sin\left(\frac{j\pi}{a}\left(x+\frac{a}{2}\right)\right)dx \quad (49)$$

where the notation of [7] has been used. From a computational point of view, we remark that these coefficients are evaluated only once, and stored in an array. Therefore, the matrix eigenvalue system (46) has to be solved for each frequency point varying only ω.

B. E-Plane Bends

The matrix eigenvalue system for the modes of the E-plane curved region is

$$\sum_{i=1}^{N}\left(\left(\omega^2\mu\epsilon - \left(\frac{r\pi}{a}\right)^2\right)P_{ij} - S_{ij}\right)d_i^{(m)} = \beta_m^{(c)2}\sum_{i=1}^{N} Q_{ij}d_i^{(m)}; \quad j = 1,2,\ldots,N. \quad (50)$$

Being the fundamental rectangular waveguide mode incident, only modes with $r = 1$ are excited in the curved region. The matrix elements P_{ij}, S_{ij}, and Q_{ij} are given by

$$P_{ij} = \frac{b}{\epsilon_i}\delta_{ij} + (1-\delta_{ij})\frac{1}{R}\frac{b^2}{2\pi^2} \times \left(\frac{(-1)^{i-j}-1}{(i-j)^2} + \frac{(-1)^{i+j}-1}{(i+j)^2}\right) \quad (51)$$

$$S_{ij} = ij\left(\frac{\pi}{b}\right)^2\left(\frac{b}{\epsilon_i}\delta_{ij} + (1-\delta_{ij})\frac{1}{R}\frac{b^2}{2\pi^2} \times \left(\frac{(-1)^{i-j}-1}{(i-j)^2} - \frac{(-1)^{i+j}-1}{(i+j)^2}\right)\right) \quad (52)$$

$$Q_{ij} = \int_{-b/2}^{+b/2}\frac{R}{y+R} \times \cos\left(\frac{i\pi}{b}\left(y+\frac{b}{2}\right)\right)\cos\left(\frac{j\pi}{b}\left(y+\frac{b}{2}\right)\right)dy. \quad (53)$$

ACKNOWLEDGMENT

The authors would like to thank A. M. Torre from Radiacion y Microondas, S.A., (RYMSA) Madrid, Spain for providing the experimental results. A. Alvarez-Melcon and D. Kinowski of ESTEC, and A. Weisshaar of Oregon State University are also acknowledged for helpful discussions and suggestions.

REFERENCES

[1] S. O. Rice, "Reflections from circular bends in rectangular waveguides-matrix theory," *Bell Syst. Tech. J.*, vol. 27, no. 2, pp. 305–349, 1948.

[2] J. A. Cochran and R. G. Pecina, "Mode propagation in continuously curved waveguides," *Radio Sci.*, vol. 1 (new series), no. 6, pp. 679–696, June 1966.

[3] C. P. Bates, "Intermodal coupling at the junction between straight and curved waveguides," *Bell Syst. Tech. J.*, vol. 48, no. 7, pp. 2259–2280, Sept. 1969.

[4] L. Lewin, D. C. Chang, and E. F. Kuester, *Electromagnetic Waves and Curved Structures*. London: Peter Peregrinus Ltd., 1977.

[5] P. L. Carle, "New accurate and simple equivalent circuit for circular E-plane bends in rectangular waveguide," *Electronics Lett.*, vol. 23, no. 10, pp. 531–532, May 1987.

[6] L. Accatino and G. Bertin, "Modal analysis of curved waveguides," *20th Eur. Microwave Conf.*, Sept. 1990, pp. 1246–1250.

[7] A. Weisshaar, S. M. Goodnick, and V. K. Tripathi, "A rigorous and efficient method of moments solution for curved waveguide bends," *IEEE Trans. Microwave Theory Tech.*, vol. 40, no. 12, pp. 2200–2206, Dec. 1992.

[8] F. Alessandri, M. Mongiardo, and R. Sorrentino, "Computer-aided design of beam forming networks for modern satellite antennas," *IEEE Trans. Microwave Theory Tech.*, vol. 40, no. 6, pp. 1117–1127, June 1992.

[9] G. Gheri and M. Guglielmi, "A CAD tool for complex waveguide components and subsystems," *Microwave Engineering Europe*, pp. 45–53, Mar./Apr. 1994.
[10] B. Gimeno and M. Guglielmi, "Multimode equivalent network representation for *H*- and *E*-plane uniform bends in rectangular waveguides," *IEEE MTT-S Int. Symp.*, Orlando, FL, May 1995, pp. 241–244.
[11] A. Alvarez and M. Guglielmi, "New simple procedure for the computation of the multimode admittance matrix of arbitrary waveguide junctions," *IEEE MTT-S Int. Symp.*, Orlando, FL, May 1995, pp. 1415–1418.
[12] W. H. Press, S. A. Teukolsky, W. T. Vetterling, and B. P. Flannery, *Numerical Recipes in Fortran*, 2nd ed. Cambridge, MA: Cambridge Univ. Press, 1992.

Benito Gimeno was born in Valencia, Spain, on January 29, 1964. He received the Licenciado degree in physics in 1987 and the Ph.D. degree in 1992, both from the Universidad de Valencia, Spain.

He was a Fellow at the Universidad de Valencia from 1987 to 1990. Since 1990 he has been Assistant Professor in the Departmento de Fisica Aplicada at the Universidad de Valencia, where he was teaching and doing research in Numerical Methods for electromagnetics. He was working at ESTEC (European Space Research and Technology Centre of the European Space Agency) under CDTI grant during 1994–1995. His current research interests include the areas of computer-aided techniques for analysis of microwave passive components and waveguide structures.

Marco Guglielmi was born in Rome, Italy, on December 17, 1954. He received the degree "Laurea in Ingegneria Elettronica" in 1979 from the University of Rome "La Sapienza," Rome, Italy, where in 1980 he also attended the "Scuola di Specializzazione in Elettromagnetismo Applicato." In 1981 he was awarded a Fulbright Scholarship in Rome, Italy, and an HISP scholarship (Halsey International Scholarship Program) from the University of Bridgeport, Bridgeport, CT, where in 1982 he obtained the M.S. degree in electrical engineering. In 1986, he received the Ph.D. degree in electrophysics from Polytechnic University, Brooklyn, NY.

From 1984 to 1986 he was Academic Associate at Polytechnic University, and from 1986 to 1988 he was Assistant Professor in the same institution. From 1988 to 1989 he was Assistant Professor at the New Jersey Institute of Technology, Newark, NJ. In 1989 he joined the RF System Division of the European Space Research and Technology Center, Noordwijk, The Netherlands, where he is currently involved in the development of passive microwave components for space application. His professional interests include the areas of solid-state devices and circuits, periodic structures, phased arrays and millimeter-wave, leaky-wave, antennas, network representations of waveguide discontinuities and microwave filtering structures.